# An Extended Multi-Phase Transport Model for Pedestrian Movement

Frank Huth Günter Bärwolff Hartmut Schwandt

*Institut für Mathematik, Technische Universität Berlin, Germany*

huth@.. baerwolf@.. schwandt@math.tu-berlin.de

April 28, 2011

**Abstract**

In this paper we present two different approaches to model multi-species pedestrian fluxes. One model is a modified single-phase fluid dynamics approach. The other model is an multi-phase transport equation model. Results of numerical experiments for the latter model are included.

## 1 Fluid- and Gas-dynamic Models

In [1] we presented a modification of Euler/Navier-Stokes equation to describe pedestrian flows. For basic information we summarize the Euler equations in the following.

### 1.1 The Euler Equations for a Two-Dimensional Pedestrian Flow

The Euler equations are obtained from the general momentum balance by making the following two assumptions which close the system of equations:

1. We consider the variable $P = P_e := \varrho\Theta I$ with $I = (\delta_{ij})_{ij} \in \mathbb{R}^{2\times 2}$ the unit or Kronecker tensor as a "pressure", which is proportional to the product of density and velocity variance. This is an analogy to the scalar pressure in fluid mechanics, and it corresponds to an ideal gas with adiabatic index $\gamma = 2$. "Traffic pressure" is regarded as the crucial quantity when we study panic situations. Energy balance then gives the term

$$-\frac{2}{\varrho}P : \nabla\vec{V} \;=\; -2\Theta I : \nabla\vec{v} \;=\; -2\Theta\sum_{ij}\delta_{ij}\frac{\partial V_j}{x_i} \;=\; -2\Theta\sum_{i}\frac{\partial V_i}{x_i} \;=\; -2\Theta\nabla\cdot\vec{V},$$

   by the definition of the dyadic product ":".

2. The heat flux density vanishes, i.e. $J = 0$.

These two assumptions lead to the Euler equations:

$$\left.\begin{aligned} \frac{\partial\varrho}{\partial t} + \nabla\cdot(\varrho\vec{V}) &= 0\,, \\ \frac{\partial\vec{V}}{\partial t} + \vec{V}\cdot\nabla\vec{V} + \frac{1}{\varrho}\nabla(\varrho\Theta) &= \vec{f}\,, \\ \frac{\partial\Theta}{\partial t} + \nabla\Theta\cdot\vec{V} &= -2\Theta\nabla\cdot\vec{V}\,. \end{aligned}\right\} \quad (1)$$

The inhomogeneity in the momentum balance is modeled as the difference between current velocity and desired target velocity, i.e.

$$\vec{f}(\vec{x},t) \;=\; \frac{1}{\tau}(\vec{V}^0(\vec{x},t) - \vec{V}(\vec{x},t)) \quad (2)$$

where $\tau > 0$ is a relaxation time.

For more details see [5, section 19.1] and [3, 4]. The challenge here is to present a meaningful analogue of the viscosity modeling for two-dimensional pedestrian flow.

### 1.2 Further extensions

Following Helbing's suggestions in [3] (for one-dimensional vehicular traffic), the target velocity $\vec{V}^0$ in the model for the forcing term in (2) in the momentum equation can be replaced by the equilibrium velocity

$$\vec{v}^e(\vec{x},t) \;:=\; \vec{V}^0(\vec{x},t) - \tau[1-p]\rho\Theta(\vec{x},t)$$

where $p$ is a probability factor, which in vehicular traffic describes the likelihood that an overtaking takes

place. In two-dimensional pedestrian flow this factor may not seem to make sense, since overtaking should be modeled by the equations themselves.

Moreover, the relaxation time may be modeled depending on the density $\varrho$, adding more non-linearity to the system.

In [3], covariance

$$C(\vec{x},t) \quad = \quad \langle(\vec{v}(\vec{x},t) - \vec{V}(\vec{x},t)$$

is introduced, namely via modification of the variance equation as

$$\frac{\partial\Theta}{\partial t} + \nabla\Theta\cdot\vec{V} \quad = \quad -2\Theta\nabla\cdot\vec{V} + \frac{2}{\tau}(C-\Theta),$$

and an additional equation for the covariance $C$, for details see [3, Equation (104)].

The model noted above contains some open questions which are deserve some further consideration. The models are derived from the mass and the momentum balance. The behavior of pedestrians follows the mass balance but not the momentum balance. This consideration leads to the investigations discussed in the next section.

## 2 The Multiphase Transport Model

Perceiving pedestrian flows as a transport problem, we start with the governing equation

$$\frac{\partial\rho_i}{\partial\vartheta} + \nabla\cdot(\rho_i v_i) = 0$$

of a transport problem, which describes the mass flow. In the sequel $\vartheta$ denotes the time, $i\in\{1,\ldots,n\}$ and $n$ is the number of pedestrian "types" or "species" distinguished by certain properties. Obviously, the desired walking direction and speed can be two most important ones of these. ones. Further, $\rho_i$ is the current density and $v_i$ the current speed of a species in a given computational domain.

The key question to be answered is what a reasonable $v_i$ for our problem is.

It turns out that $v_i = v_i(\rho_i,\ldots)$ is necessary for realistic cases which means that the problem is nonlinear and carries both the analytical and numerical challenges of equations of that type.

## 3 Two-Dimensional $n$-Species Model Derived from One-Dimensional One-Species Model

Starting from the viewpoint of [2], we recommend an extension. In that paper the governing laws are stated as follows:

$$\begin{aligned}
\rho &= \sum_{i=1}^{n}\rho_i\ , \\
\frac{\partial\rho_i}{\partial\vartheta} + \nabla\cdot F_i(\rho) &= \epsilon\Delta\rho_i\ , \qquad (3)\\
F_i(\rho) &= a_i\rho_i V(\rho) d_i\ , \\
V(\rho) &= 1-\rho\ , \qquad (4)
\end{aligned}$$

with $\rho_i\in[0,1]$ the species' density; $\rho\le 1$ total density of the species; $F_i$ flux functions; $\epsilon$ a small positive constant (preferably zero, the default for our simulations); $a_i>0$ constants; $V\in[0,1]$ velocity-magnitude (other ideas for (4) are in stock); $d_i$ given species-specific direction unit-vector fields.

An important to be answered is which boundary conditions apply. Boundary conditions, that have been applied so far are:

$\rho_i$ **Walls** zero gradient meaning that space up to walls will be used if needed

**Entrances** (random) fixed value meaning that a (time-varying) pedestrian density is up to enter the computational domain; this pure behavior has to be adapted in a way to prohibit entrance in case that the interior of the computational domain is at that point already (over)crowded

**Exits** zero fixed value meaning that pedestrians vanish unimpededly by members of their own species through the exit

$\rho$ **Walls, Entrances, Exits** zero gradient extending the total density information up to the boundaries

$V$ **Walls, Entrances, Exits** fixed value (e.g. $1-\rho$) naturally extending the congestion inclination up to the boundary this way

$d_i$ **Walls** zero fixed value meaning that walking through walls is not possible

**Entrances** inward-facing normal unit vectors to provide for direct entrance

**Exits** outward-facing normal unit vectors providing direct exit

Some of the properties of this model are:

- extensible two-species model
- time-static direction for each species
- non-resolving frozen patterns in case of larger densities because $\rho = 1 \Longrightarrow V = 0$, if $\epsilon = 0$
- a system of coupled ODEs
- $\rho_i = 0$ poses no problem (to our knowledge)
- like blind persons with canes in hand, who stick to their planned direction

# 4 Density-Gradient Driven-Direction and Speed Modifications

The model in section 3 lacks a mechanism to avoid running blindly into congestions and to quick solution of this. To alleviate this freezing tendency of the model without too much relying on using the $\epsilon\Delta\rho_i$-term we have considered a new term $G_i(\rho)$ in dependence of density gradient.

The model should reflect the behavior of a blind person, who tries to stick to the planned direction, but due to the congestion ahead the person is forced to change the plan.

Therefore the model takes the following form:

$$\frac{\partial \rho_i}{\partial \vartheta} + \nabla \cdot F_i(\rho) + G_i(\rho) = \epsilon \Delta \rho_i$$

Concerning boundary conditions several considerations have been attempted. One idea for entrances and exits is to follow the ideas presented in section 3. That would imply a membrane-like effect, permitting inflow at entrances only but no back-flooding if the interior is too crowded. Since this would break the underlying laws of the model at these faces, the decision was made to allow back-flooding too.

For the following models $b_i$ is a positive constant.

## 4.1 Simple Gradient Terms

The ansatz

$$G_i(\rho_1, \ldots, \rho_n) := -b_i \nabla \cdot (\rho_i \nabla \rho) \qquad (5)$$

is the usual transport term for $\rho_i$ with the transport velocity $-b_i \nabla \rho$.

An idea to modify (5) is to go one step back - and use the self-transporting total density (like a one-species model) and weight this by the proportion of the phase considered. This yields:

$$G_i(\rho_1, \ldots, \rho_n) := -b_i \frac{\rho_i}{\rho} \nabla \cdot (\rho \nabla \rho) \qquad (6)$$

This and that the flow occurs in the desired direction and the factor $\frac{\rho_i}{\rho}$ ensure the right amount of flux. The latter factor poses no problem analytically but has to be taken care of numerically.

These terms share the undesired property, to permit unlimited walking speeds and thus do not fit well into the framework of [2]. In consequence, we propose a modification of the gradient term.

## 4.2 A Strategic vs. Tactic Decision Making Approach

Following (3), let us consider the equation

$$\frac{\partial \rho_i}{\partial \vartheta} + \nabla \cdot F_i(\rho_1, \ldots, \rho_n) = 0 \,,$$

with

$$F_i(\rho_1, \ldots, \rho_n) = \rho_i V d_i^{(s)} \,.$$

Here $d_i^{(s)}$ denotes the direction unit-vector field giving a desired (strategic) walking direction. $V$ denotes just the magnitude of the speed in that direction. This models a throttling-capabilty sticking to one path by walking along the (locally given) directions.

The heuristics which might be introduced at this point, is to perceive $V$ as the chance to follow the strategic goal of reaching a certain destination on a desired path, which then can be augmented by alternatively taking a tactical decision to avoid densely populated areas.

To put these two ideas together we may choose an alternative (tactical) direction (unit-)vector field $d_i^{(t)}$ and weighting it with a strategic-chance-depleted term $(1 - V)$. This gives us the missing part of a partition of unity $V + (1 - V)$.

In this way we divide the direction and speed decision into

$$\begin{aligned} F_i^{(s)} &= \rho_i V d_i^{(s)} \,, \\ F_i^{(t)} &= \rho_i (1 - V) d_i^{(t)} \,, \end{aligned}$$

quite naturally.

The choice

$$d_i^{(t)} = \begin{cases} -\nabla\rho / |\nabla\rho| & \text{for } |\nabla\rho| > 0 \\ 0 & \text{for } |\nabla\rho| = 0 \end{cases}$$

should be a natural one too. But, what clearly is to be noted, is that $d_i^{(t)}$ is discontinuous where $|\nabla\rho| = 0$ is true. This behavior is in accordance with the observation, that pedlock occurs rather suddenly and the fact that indeed $d_i^{(t)} = d^{(t)}$ holds reflects the fact, that strategic goals have to be neglected in favor of tactical goals if high densities are reached.

Assembling the parts and introducing constants $a_i$ and $b_i$ for greater flexibility give:

$$\frac{\partial\rho_i}{\partial\vartheta} + \nabla\cdot\left\{\rho_i\left[a_i V d_i^{(s)} - b_i\left(1-V\right)d_i^{(t)}\right]\right\} = 0$$

or

$$\frac{\partial\rho_i}{\partial\vartheta} + \nabla\cdot\left\{\rho_i\left[a_i\left(1-\rho\right)d_i^{(s)} - b_i\rho d_i^{(t)}\right]\right\} = 0 \qquad (7)$$

with $V = 1-\rho$.

Another problem obviously present with the term $F_i^{(t)}$ is that it acts most vigorously where the density is high. This might lead to the violation of the condition $\rho, \rho_i < 1$ because of numerical overshooting. Hence another risk to be expected is numerical oscillation of the solution (which might be interpreted as remaining untargeted pedestrian activity at high densities).

# 5 Model Modification by Involvement of Environmental Information

The models discussed so far, do not reflect the ability of pedestrians to take environmental information far from a current pedestrian position into account. This information can be considered as part of the strategic goals modeled by the $d_i^{(s)}$ terms in (7) for instance.

The idea how to involve environmental information is to create a potential field caused by far field information like geometry of the considered region, congestions, stairs, and by local information of pedestrians without any congestion.

This model component can be described by $j$ equations per pedestrian species $i$ (reflecting $j$ different influences) of the form

$$\alpha_j^{(i)}\Delta\phi_j^{(i)}(\vartheta) = f_j^{(i)}(\vartheta)\ , \qquad (8)$$

where $\alpha_j^{(i)}$ are constants which give a global information weighting and $f_j^{(i)}(\vartheta)$ are source terms derived from local environmental information, for example the density $\rho_k(\vartheta)$ of any pedestrian species.

This gives us a pedestrian-specific potential sum by $\phi_i(\vartheta) = \sum_j \phi_j^{(i)}(\vartheta)$. The vector field

$$d_i^{(s)}(\vartheta) = \frac{\nabla\phi_i(\vartheta)}{|\nabla\phi_i(\vartheta)|}$$

gives a prefered (strategic) moving direction. For points with $|\nabla\phi_i(\vartheta)| = 0$ a random direction could be chosen.

# 6 Numerical Application

Numerical experiments have been done for the terms proposed in the sections 4.1, 4.2 and 5.

## 6.1 Open Field Operation And Manipulation (OpenFOAM)

The OpenFOAM library and tools have been chosen owing to their following properties:

- finite volume method toolbox
- primarily a C++ library for field operations $\Longrightarrow$ conceptually open (but most stuff is physics-related, especially with fluxes of all kinds in mind)
- open source $\Longrightarrow$ fully accessible
- many built in preprocessing solver and post-processing utilities already implemented
- recommended adaption strategy is to copy a solution similar to the own problem and to extend/adapt that code
- extremely powerful and flexible against the price of code complexity
- it is e.g. capable of handling convex cells with arbitrarily shaped polygons as faces

The most important reason for the use of a finite volume method consists in the preference to produce results that are as good as achievable coherent with reality to the goal of doing math theory. This has led to the conclusion, that the good mass-preservation properties of a finite volume method and the flexibility in flux modeling can't be matched by for instance a finite element method.

## 6.2 Some Considerations for the Implementation

The properties of the equations do require thorough considerations of many aspects of the implementation.

#### 6.2.1 Mesh

For faithful implementation of the equations of Section 3 in a finite volume scheme it is crucial to use a mesh, which is aligned to the $d_i$-fields to avoid numerical "diffusion" (this might be impossible if the fields of different species do not permit to do so).

#### 6.2.2 Boundary Conditions

The $V$ and $\rho_i$ entrance `fixedValue`-patches have to be modified to ensure that no further influx into an already crowded cell or out-flux from an already empty cell takes place.

Another notable example in this field is that the `grad()`-method of OpenFOAM silently applies `zeroGradient` boundary conditions to the resulting field, so that any e.g. `fixedGradient` of the input field is ignored in the produced gradient field. However, the provision of a scheme respecting the given `fixedGradient` of the input field does not take much more than changing a `zero` into a `calculated` at the right place, because the rest of the implementation is already provided by OpenFOAM.

#### 6.2.3 Interpolation

Interpolation is the operation to somehow procure values at cell faces, where usually no values are stored by the schemes implemented in OpenFOAM.

Due to the nature of the problem, strict upwind has proved to be the most secure way to ensure the $[0, 1]$-boundedness of the variables concerned. Special care with respect to that has to be taken at boundaries because no interpolation takes place there and so the upwind-idea is corrupted at these patches. This is especially true for the back-flooding idea from Section 4. Therefore, a modified version of boundary conditions and/or interpolation schemes has to be provided.

#### 6.2.4 Examples of Numerical Issues

For the model of Section 4.2, the nonlinear loop in most of the time-steps for the tested cases did not converge for both of the tested values $b_i \in \{0.5, 1\}$ after 100 iterations. Because no unbounded values have been observed, the probable cause is oscillation (see remark concerning (7) below).

Implementing (7) implies the risk of a numerical division by zero. The convenient way to use $\frac{\nabla\rho}{|\nabla\rho|} \approx \frac{\nabla\rho}{|\nabla\rho|+\mathrm{SMALL}}$ has been chosen. This smoothens the discontinuity of the term and SMALL can be chosen in a way to dampen numeric overshooting, too.

Several ideas have been tried to split the gradient term of (6) into an explicit and an implicit part in order to apply Crank-Nicholson like schemes, as there is for instance:

$$\underbrace{\nabla \cdot (\rho \nabla \rho_i)}_{(*)} + \underbrace{\nabla \cdot (\rho \nabla (\rho - \rho_i))}_{(**)} ,$$

where $(*)$ is to be used partially explicitly and implicitly and $(**)$ solely explicitly.

But the simple explicit use of the whole term produced the best results with respect to the preservation of the $\rho \in [0, 1]$ requirement without having explored much of the interpolation schemes provided by OpenFOAM.

Another implementation detail considered concerning (5) is that OpenFOAM has a built in implicit $\nabla \cdot (\rho \nabla \rho_i)$-term but no implicit $\nabla \cdot (\rho_i \nabla \rho)$-term. A solution considered (and tested) is to divide the operator into OpenFOAM-known parts:

$$\begin{aligned} \nabla \cdot (\rho_i \nabla \rho) &= \nabla \cdot (\rho_i \nabla \sum_j \rho_j) \\ &= \underbrace{\nabla \cdot (\rho_i \nabla \rho_i)}_{(*)} + \underbrace{\nabla \cdot (\rho_i \nabla (\rho - \rho_i))}_{(**)} \end{aligned}$$

which gave us two operators which OpenFOAM knows. Here (as above) $(*)$ might be used partially implicitly. But this solution had been replaced by the use of a single flux field containing the flux of this term, too.

## 7 Numerical Experiments

### 7.1 Model with Simple Gradient Terms

To illustrate the effects of the newly introduced term, some of the results have been chosen from the setup following (7).

The chosen setup is two species in a computational domain of $[-1, 1]^2$ with all boundaries being walls. The initial values $\rho_1 = 0.4 \pm 10\%$ and $\rho_2 = 0.35 \pm 1.5\%$ are pretty densely populated, leading to freeze up with the model from Section 3. Though all the chosen examples $a_i = 1$ has been used.

The observable checkerboard patterns for the $b_i \neq 0$ cases consists of moving patches which are larger than the cells of the mesh used for the implementation, so they should reflect a model property rather than an implementation problem.

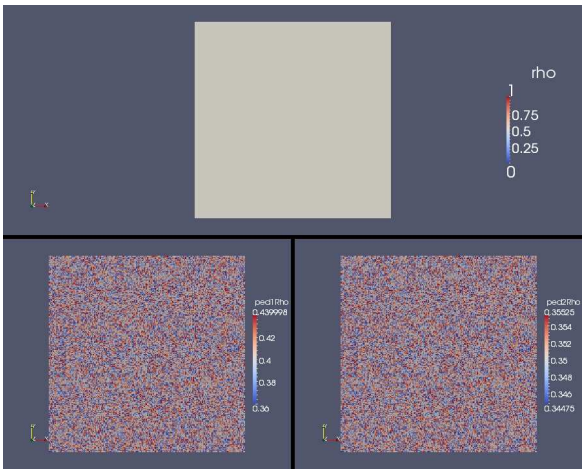


Figure 1: Initial Values for Tests with Model of Section 4.2

Figures 2 through 5 show some time steps for several parameter constellations given in table 1. The initial values are shown in figure 1, where $\rho = \sum_i \rho_i$ is not yet calculated.

| $d_1^{(s)}$ | $d_2^{(s)}$ | $b_1$ | $b_2$ | fig. |
|---|---|---|---|---|
| (1,0) | (-1,0) | 0 | 0 | fig. 2 |
| (1,0) | (-1,0) | 1 | 1 | fig. 3 |
| (1,0) | (0,1) | 0 | 0 | fig. 4 |
| (1,0) | (0,1) | 0.5 | 0.5 | fig. 5 |

Table 1: Parameter configuration

Figure 2 illustrates the development from the state of Figure 1 to frozen state for the 180° encounter with only throttling capability enabled. No significant development takes place between the last two time steps shown.

Figure 3 illustrates the development from the state of Figure 1 to the complete species separation for the 180° encounter with throttling and gradient-term enabled. Some amount of numerical overshooting has to be noted, too.

Figure 4 illustrates the development from the state of Figure 1 to frozen state for the 90°-encounter with only throttling capability enabled. No significant development takes place between the last two time steps shown.

Figure 5 illustrates the development from the state of Figure 1 to mostly species separation for the 90° encounter with throttling and gradient-term enabled. The trial had been canceled due to a lack of time and disk space. So further separation may well be expected. Some amount of numerical overshooting has to be noted, too.

### 7.2 Model with Involved Environmental Information

The setting for this model is slightly more complex (as to be seen in Figure 6). The idea has been to take the initial value distribution law for the two species $\rho_{1.2}$ of Section 7.1. The computational domain is provided with two exits (one at the south half of the west boundary and one at the north half of the east boundary).

The potentials are generated in the following way:

- $\rho_1$ is attracted by both exits and $\rho_2$ only by the former one,
- both species are repelled by $\sum_i \rho_i > 0.8$ (weighted by the $\alpha_{\text{jamAttraction}}$-parameter).

The gradient term used has been according to (5)

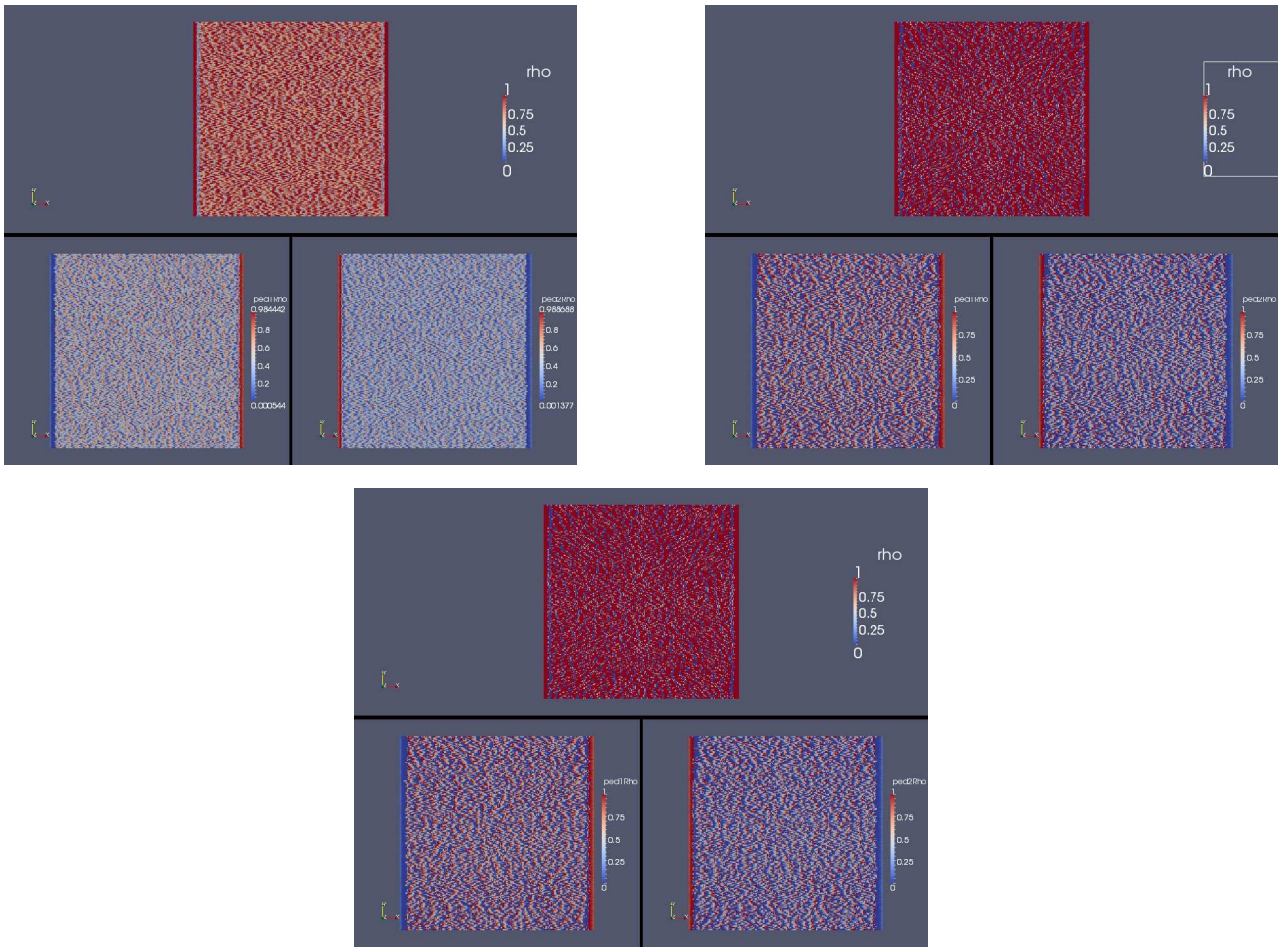


Figure 2: Time Steps 0.25098, 189 and 378 of Tests with Model of Section 4.2: 180° Encounter, Throttling only

and the parameters have been set as follows:

$$\begin{aligned}
\epsilon &= 0 \\
a_1 &= 1 \\
a_2 &= 3 \\
b_1 &= 0.1 \\
b_2 &= 0.3 \\
\alpha^{(1)}_{\text{jamAttraction}} &= -.005 \\
\alpha^{(2)}_{\text{jamAttraction}} &= -.005 \\
\rho_1(\vartheta = 0) &= 0.4 \pm 10\% \\
\rho_2(\vartheta = 0) &= 0.35 \pm 1.5\%
\end{aligned}$$

Figure 6 depicts the situation starting at time 0 (where the potential field is yet undefined) and ending at time 308. There the information for species 1 and 2 is shown on the left and right, respectively. The upper field shows the density of the species and the lower field the $d_i^{(s)}$ fields colored by $\phi_i$.

The "pushed to the edge effect" of species 2 in the east half of the domain can be avoided by better choices of the $\alpha^{(i)}_{\text{jamAttraction}}$.

## References

[1] G. Bärwolff, M.-J. Chen, and H. Schwandt. Automaton model with variable cell size for the simulation of pedestrian flow. In E. Y. Li, editor, *Proceedings of the 7th International Conference on Information and Management Sciences 2008 (IMS 2008, 12–19 August 2008, Urumtschi, China)*, pages 727–736. California Polytechnic State University Press, Series of Information and Management Sciences, Vol. 7, Pomona, California, 2008.

[2] St. Berres, R. Ruiz-Baier, H. Schwandt, and E. M. Tory. A multiresolution finite volume method for

pedestrian flow at a crossing. *AIMS' Journals,*, 2010.

[3] D. Helbing. Theoretical foundation of macroscopic traffic models. *Physica A*, 219:319–407, 1995.

[4] D. Helbing. Gas-kinetic derivation of navier-stokes-like traffic equations. *Physical Review E*, 53:2366–2381, 1996.

[5] D. Helbing. *Verkehrsdynamik: Neue physikalische Modellierungskonzepte*. Springer-Verlag Berlin Heidelberg, 1997. ISBN 3-540-61927-5.

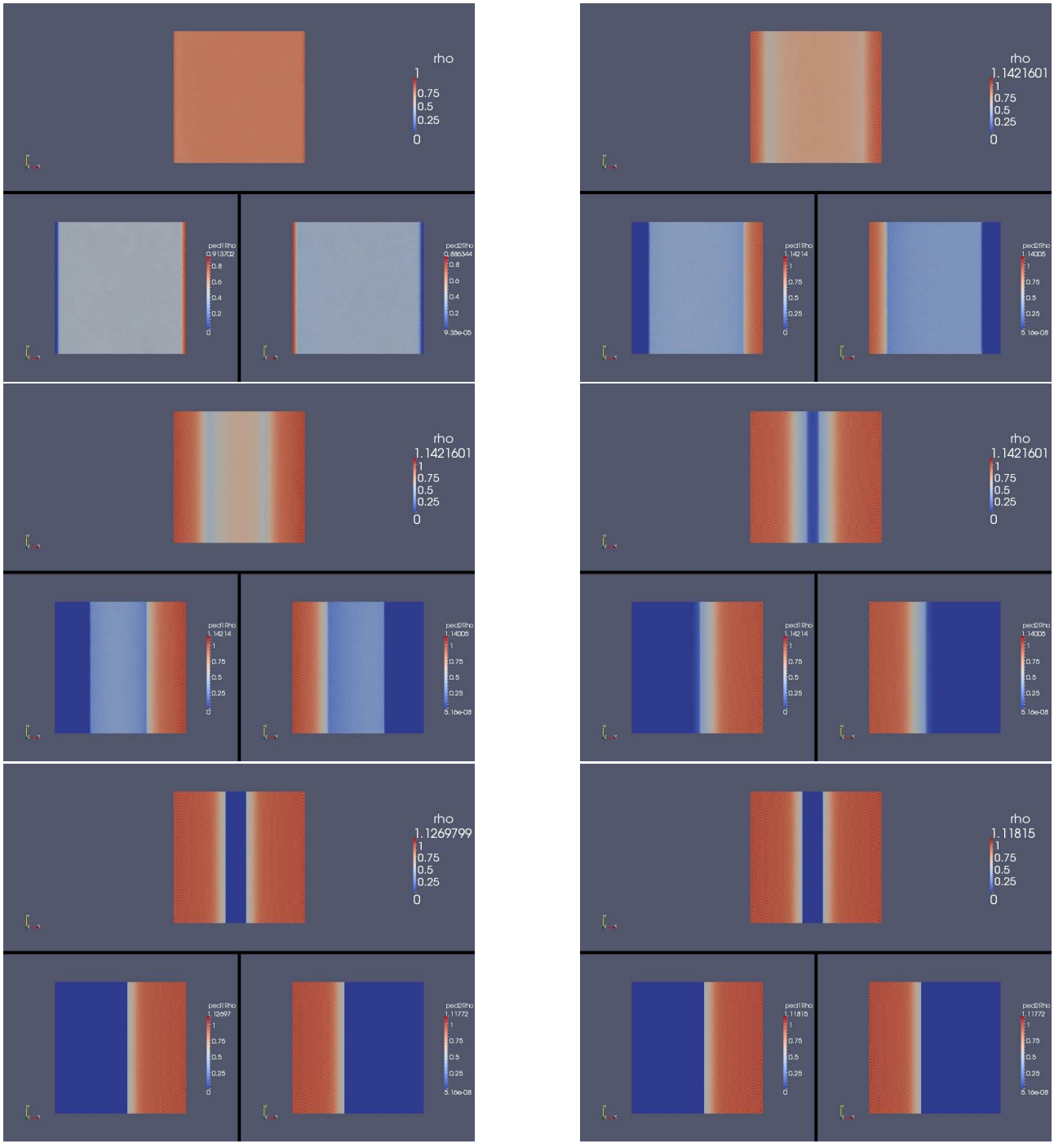


Figure 3: Time Steps 0.250213, 1.24988, 2.49993, 3.75024, 9.99977 and 19.9998 of Tests with Model of Section 4.2: 180° Encounter, Throttling plus Gradient-Term

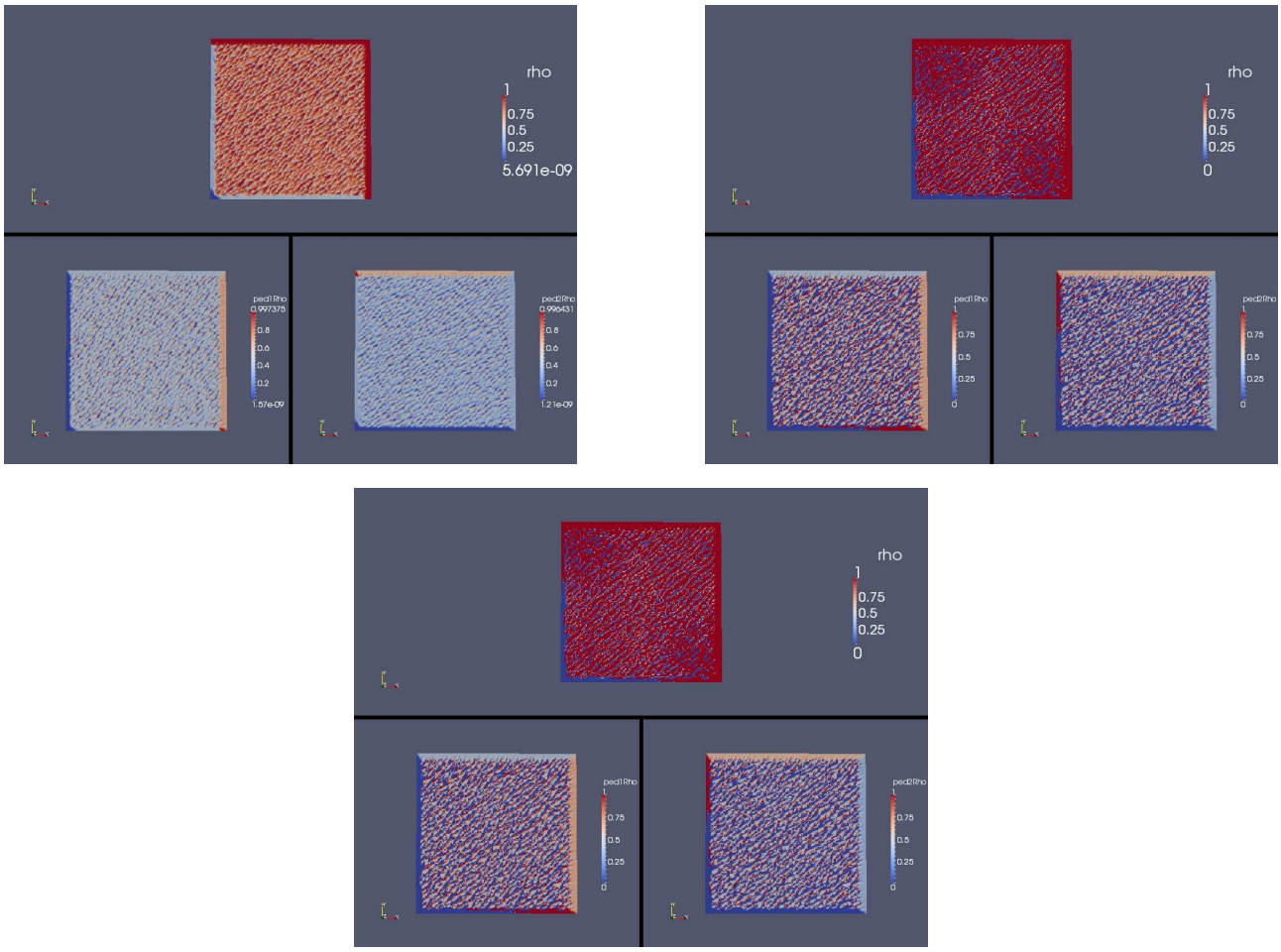


Figure 4: Time Steps 0.249799, 384 and 768 of Tests with Model of Section 4.2: 90° Encounter, Throttling only

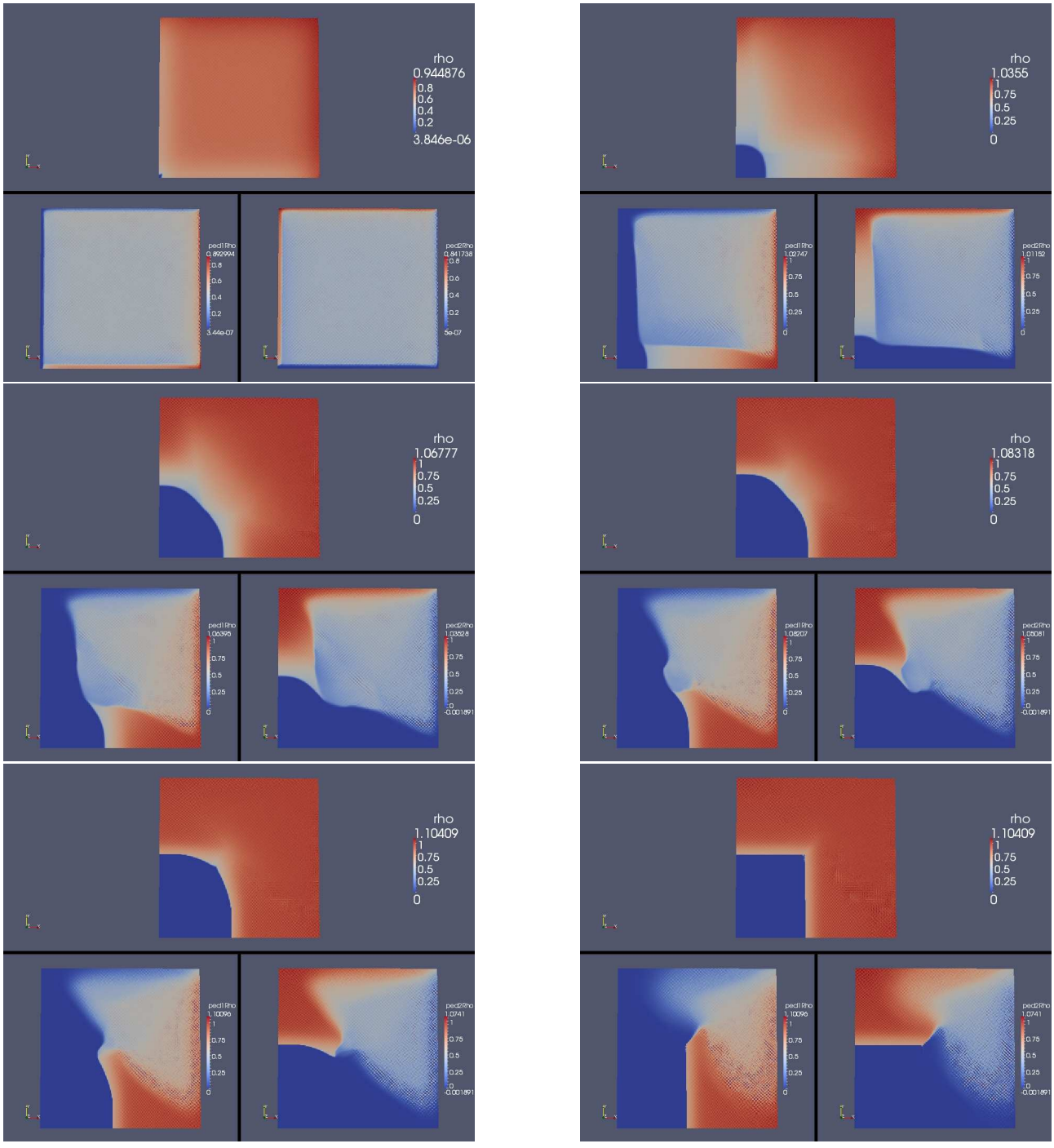


Figure 5: Time Steps 0.250246, 1.24979, 2.49979, 3.74979, 4.99979 and 15.4998 of Tests with Model of Section 4.2: 90° Encounter, Throttling plus Gradient-Term

Figure 6: Equidistant Time Steps from 0 to 308 of the Pedestrian Flow Model Influenced by Potentials